BNL-81971-2009-IR

C-A/AP/#343
January 2009

Multipacting simulation study for 56 MHz Quarter Wave Resonator using 2D code

D. Naik, I. Ben-Zvi

Collider-Accelerator Department
Brookhaven National Laboratory
Upton, NY 11973

Multipacting simulation study for 56 MHz Quarter Wave Resonator using 2D code

Damayanti Naik, Ilan Ben-Zvi

Abstract

A beam excited 56 MHz Radio Frequency (RF) Niobium Quarter Wave Resonator (QWR) has been proposed to enhance RHIC beam luminosity and bunching. Being a RF cavity, multipacting is expected; therefore an extensive study was carried out with the Multipac 2.1 2D simulation code. The study revealed that multipacting occurs in various bands up to peak surface electric field 50 kV/m and is concentrated mostly above the beam gap and on the outer conductor. To suppress multipacting, a ripple structure was introduced to the outer conductor and the phenomenon was successfully eliminated from the cavity.

1. Introduction: Multipacting, a highly probable phenomenon in all RF structures, is an electron avalanche phenomenon caused by resonating electron multiplication due to secondary emission [1, 2]. Starting from the walls or inside the cavity, the electrons gain energy from the RF field and follow a repetitive path. As the electrons hit the cavity wall, and depending on the secondary yield of the wall's material, they accumulate in greater numbers thus creating an electron cloud. The cloud absorbs much of the power pumped into the system and prevents the structure from functioning at its full capacity. The impacts of the electrons on the cavity wall raise its temperature, this fact is important for superconducting material as it may quench superconductivity. Symmetry in RF structures also increases the probability of multipacting. The 56 MHz Quarter Wave Resonator (QWR) [3], (shown in Fig. 1) has a symmetrical structure, made up of the superconducting material niobium, and thereby susceptible to sever multipacting [2]. A brief simulation of this process in the cavity was therefore carried out with both 2D and 3D code. However, at first, simulation was carried out without coupler and dampers in the cavity with Multipac 2.1 2D code [4] and the present article discusses the results and a method to suppress multipacting in this cavity.

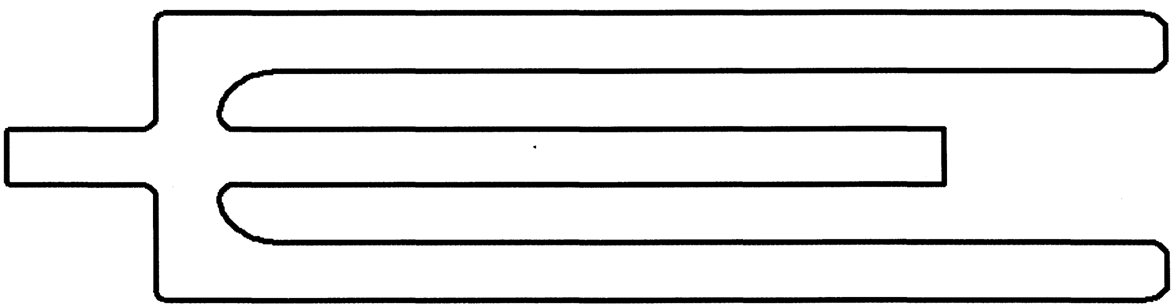

Fig. 1. The outline of the 56 MHz RF Quarter Wave Resonator in 2-Dimension without coupler and dampers.

2. Simulation code features: Linux based Multipac 2.1 2D code, works for axial symmetric RF structure. Without coupler and dampers, the cavity has an axial symmetric geometry, hence the Multipac 2.1 code can be employed in this problem. Based on the Finite Element Method field solver, the code calculates the time harmonic electromagnetic field. Thereafter it locates multipacting field levels, aided by data on the secondary yield of the cavity material (Fig. 2 shows the secondary yield from Niobium.). Finally, it details the resonant trajectories of the electrons. For this entire operation, and to display the results, the code uses MATLAB graphical user interface.

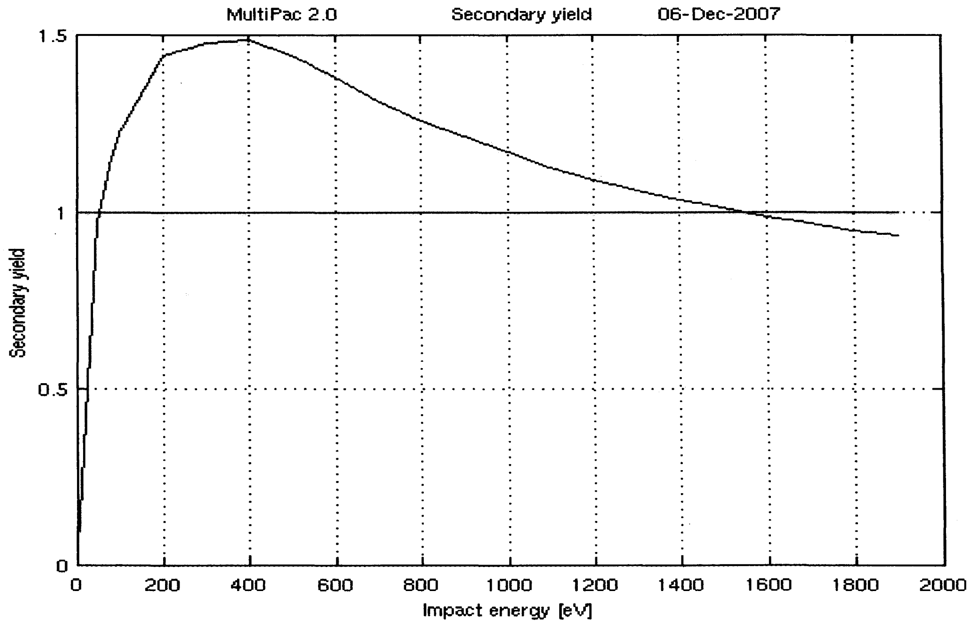

Fig. 2. Secondary yield for Niobium as a function of the electron impact energy in eV.

The representation of the multipacting in the cavity is derived mainly from three outputs (called Triplot). The counter function; C_N/C_0 viz. ratio of the total number of free electrons after N impacts to the initial number of electrons, the final impact energy of the electrons after N impacts; $E_{fN,}$ and the enhanced counter function; $e_N/C_{0,}$ i.e. ratio of the total number of secondary electrons after N impacts to the initial number of electrons. The code states that if the enhanced counter function > 1 or the final impact energy of the electron after 20 impacts is in the band of secondary emission coefficient larger than 1, then multipacting is probable at that field level. However, to confirm the severity of the occurrence, 100 impacts with an enhanced counter function greater than or equal to 10^5 was adopted as a significant multipacting level for the present study.

3. Simulation: In the cavity, the peak surface electric and magnetic field rise up to 44.19 MV/m and 1054 gauss with the maximum electric field at the gap and the magnetic field at end of the cavity (Fig. 3) for 2.5 MV accelerating voltage across the gap. With 2 eV initial energy of the electron, 5 degree RF phase interval and 1 kV/m electric field step the simulation was carried out for the entire geometry. However, the cavity's (length of the cavity is 154.57 cm with outer diameter 25 cm) volume seems to be quite large for single run with the chosen parameters. Therefore, full geometry was scanned in a number of runs taking a small portion of the cavity at a time.

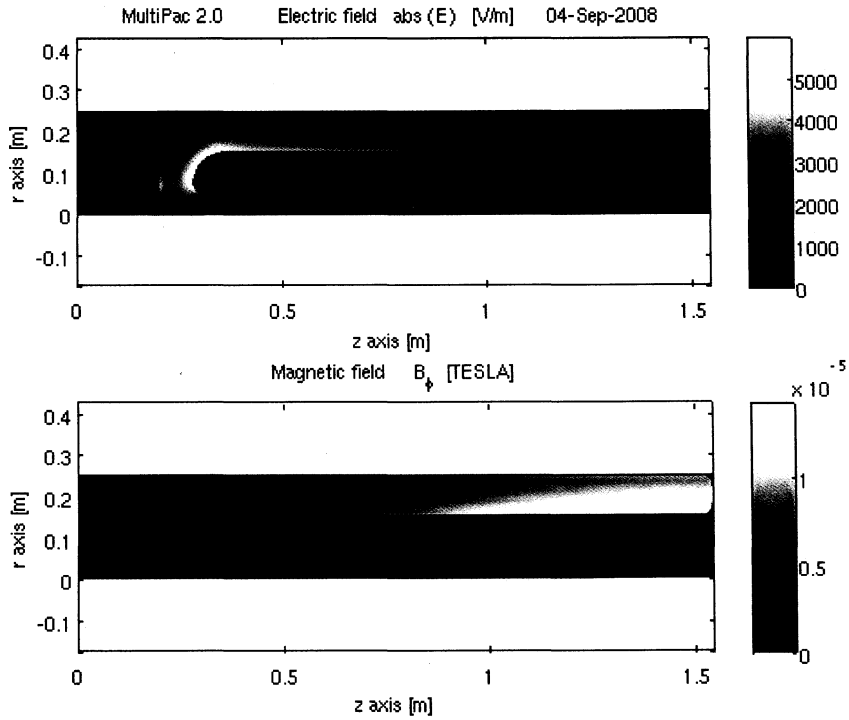

Fig. 3. Distribution of the electric and magnetic field in 56 MHz QWR cavity.

The results are as expected. Both single-point and two-point multipacting are found. They are concentrated mostly at the cavity's top corner, above the beam gap and on the outer conductor covering more than half the length of the cavity and showing a tendency to move towards the closed end of the cavity. For 20-40 cm of the cavity, (i.e top corner and above the beam gap) both types of multipacting occur. The simulation outputs' is shown in Fig. 4. The blue highlighted zone in Fig. 4a is the location where electrons are emitted with energy 2 eV,

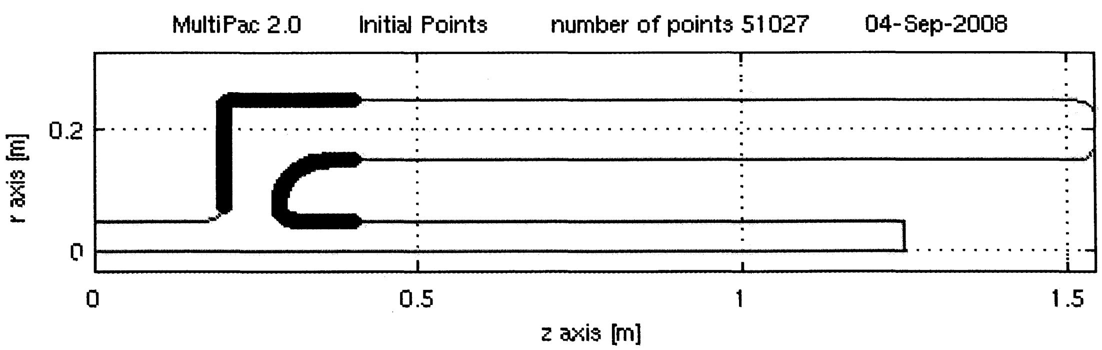

Fig. 4a. Points between 20-40 cm where initial electrons were generated to cause multipacting.

phase 0- 360 degree and mold to the resonant trajectory by the electric and magnetic field. The Fig.4b, the triplot, for the indicated zone shows the counter function, average electron energy after 100 impacts and enhanced counter function. Enhanced counter function in Fig. 4b. reveals that multipacting occurs at peak surface electric field level 25, 31, 35-37 and 47 kV/m. The electron trajectories at different locations of the cavity are shown in Fig. 4c, 4d, 4e, 4f. At 25 and 47 kV/m single-point multipacting takes place on the outer conductor whereas for the 31 kV/m two-point multipacting concentrates on the top corner of the cavity. However, for 35 kV/m, the trajectories are of the two-point multipacting variety, moving away from the gap zone and toward the end of the cavity.

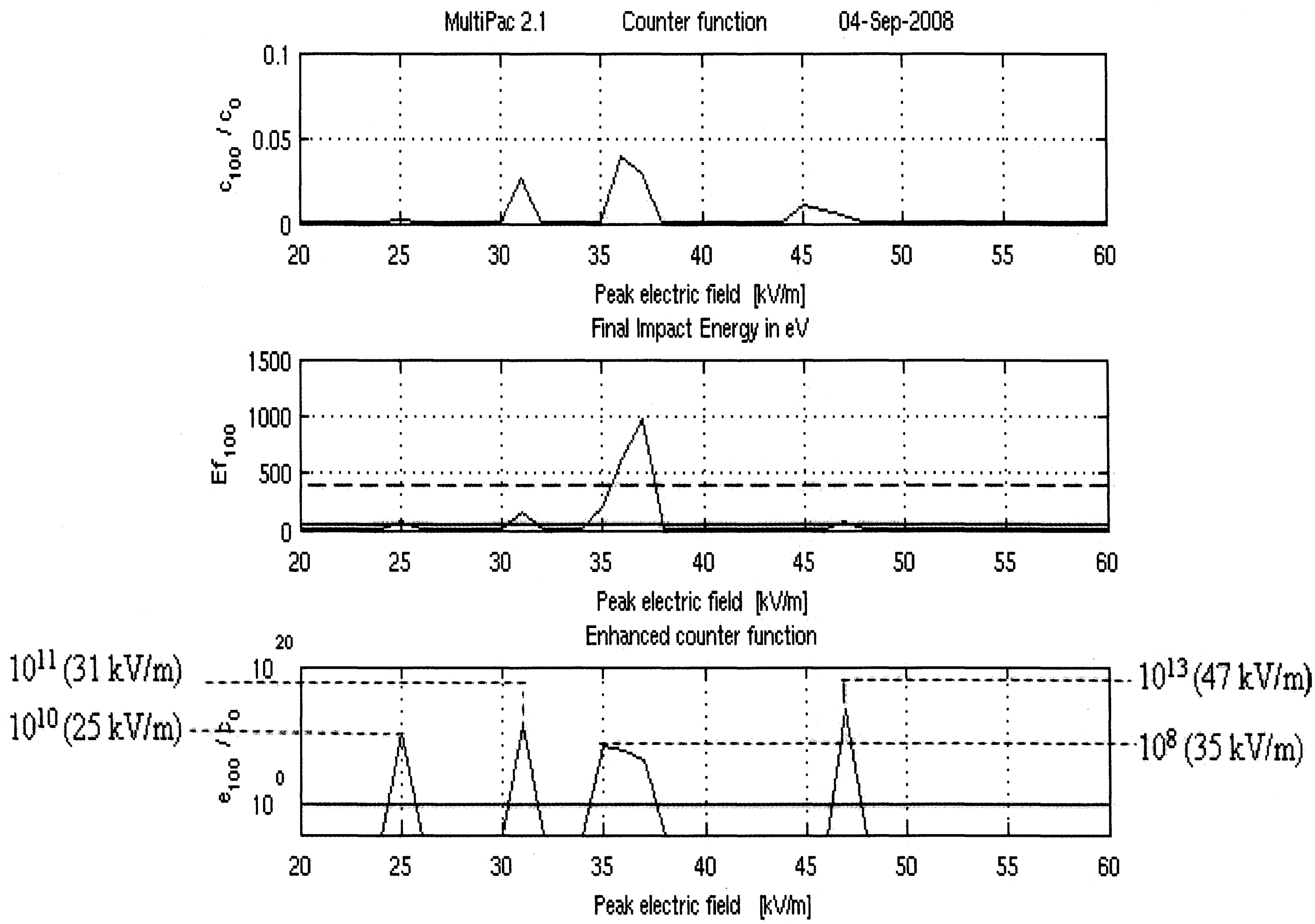

Fig. 4b. Triplot showing counter function (top), the average final energy (middle) and the enhanced counter function (bottom) for 100 electron impacts.

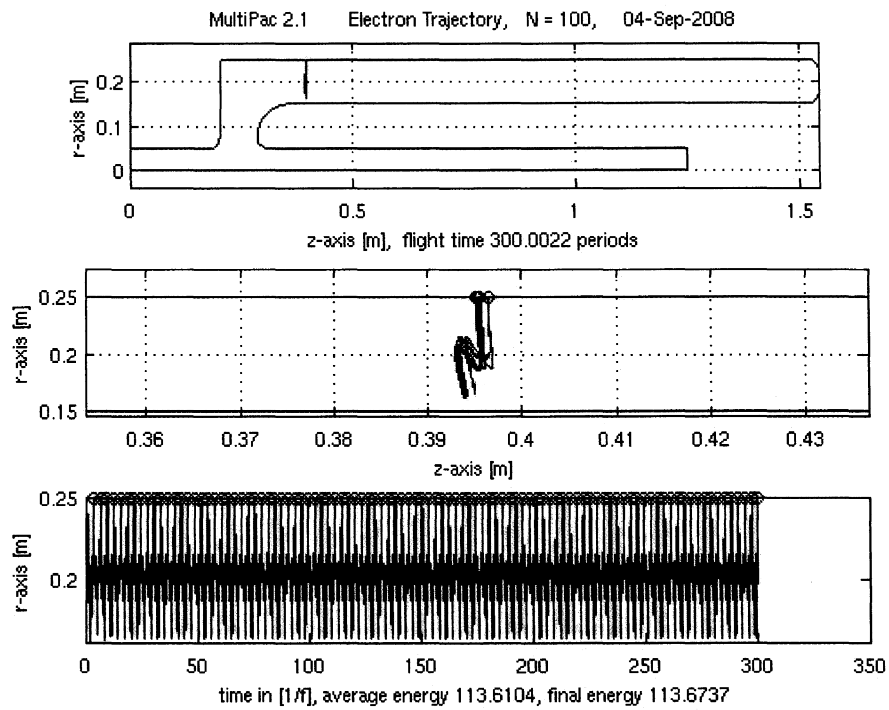

Fig. 4c. Electron trajectory in single-point multipacting at 25 kV/m. The top figure represents the trajectory of the electron in (r, z) coordinates, the middle one is an expanded plot of a part of the top one, and the bottom plot illustrates the electron trajectory in (r, t) coordinates where t is the time in periods. The circles indicate the impacts on the walls of the cavity.

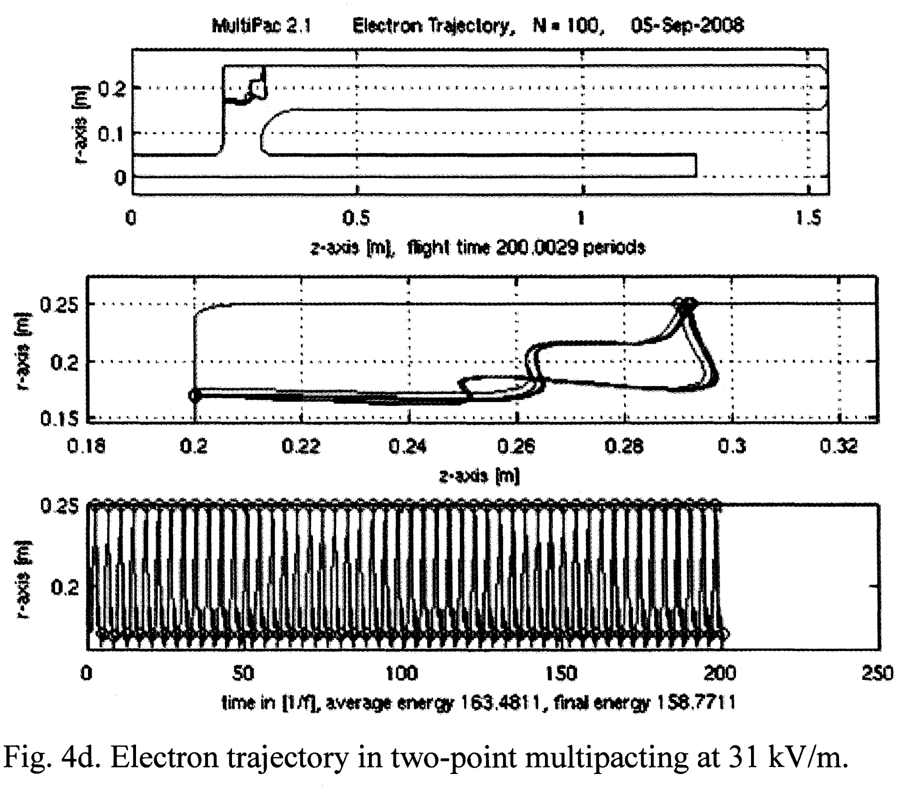

Fig. 4d. Electron trajectory in two-point multipacting at 31 kV/m.

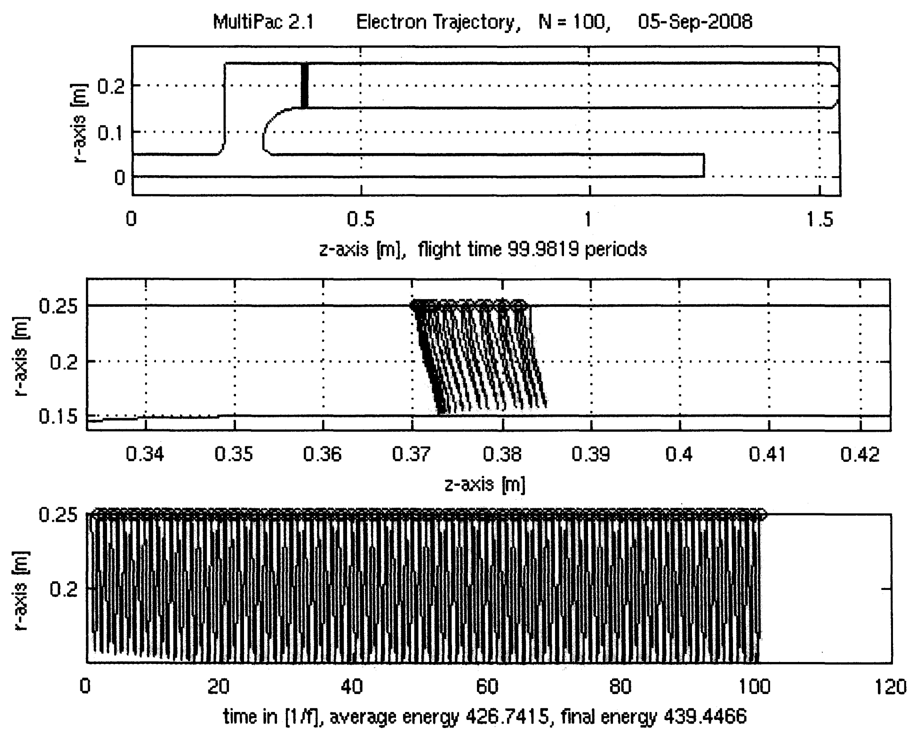

Fig. 4e. Electron trajectory in single-point multipacting at 47 kV/m.

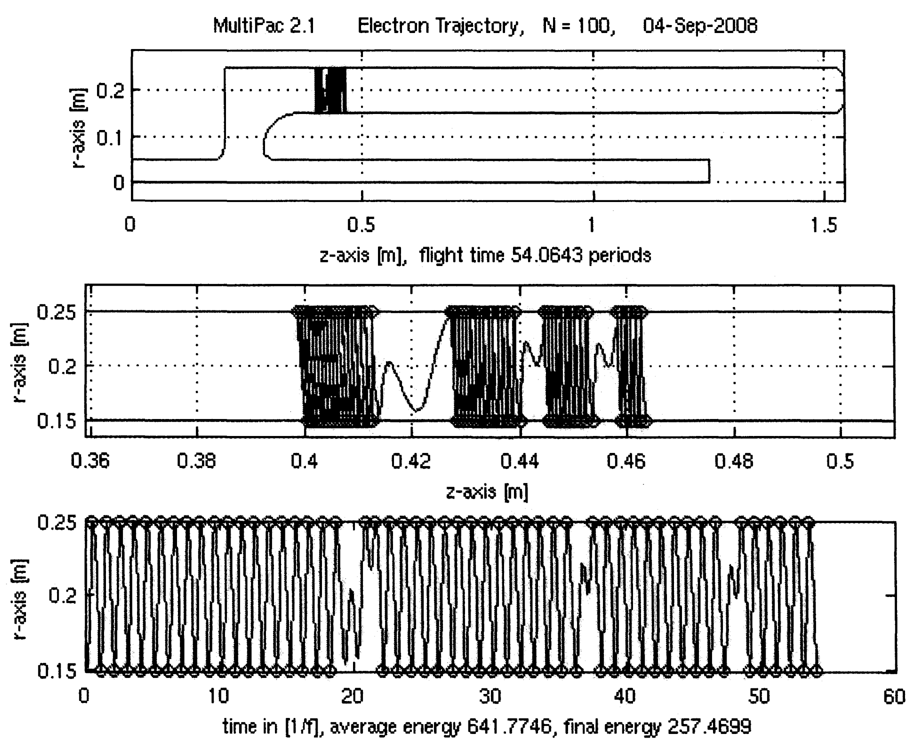

Fig. 4f. Two-point multipacting electron trajectory at 35 kV/m showing a tendency to move towards the end of the cavity.

The outputs from the rest of the cavity also exhibit that, electrons generated from both the inner and outer conductor are capable of carrying out multipacting. However, irrespective of their point of origin, they impact on the outer conductor in single-point multipacting whereas both on inner and outer conductor in two-point multipacting (Electron generated on the inner conductor at first moves towards the outer conductor and undergo single-point or two-point multipacting). In all cases they keep on moving towards the end of the cavity. The electron trajectories (for the rest of the cavity) are shown in the Fig. 5a, b, c, d, e, f. They cover up to 101 cm (including the beam pipe) which is 81 cm from the beam gap end of the outer conductor (up to more than half on it). From the figure it is clearly visible that electrons travelling from the outer conductor to the inner conductor do not necessarily follow the same path while reversing their direction; this accounts the different field strengths experienced by the electrons during their back and forth oscillation. Peak surface electric field up to 50 kV/m favors these trajectories.

(a)

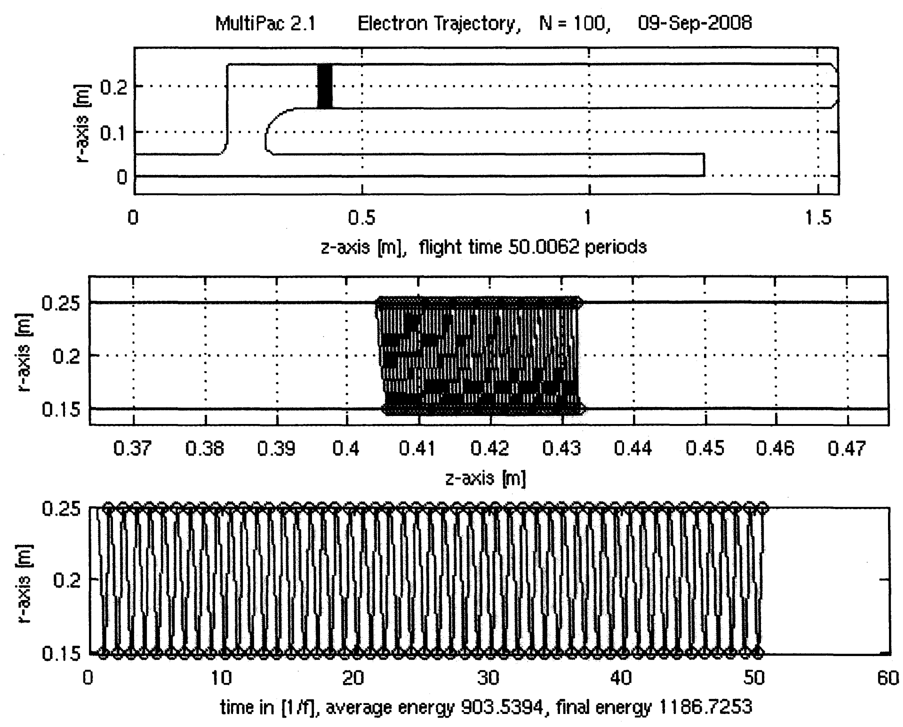

(b)

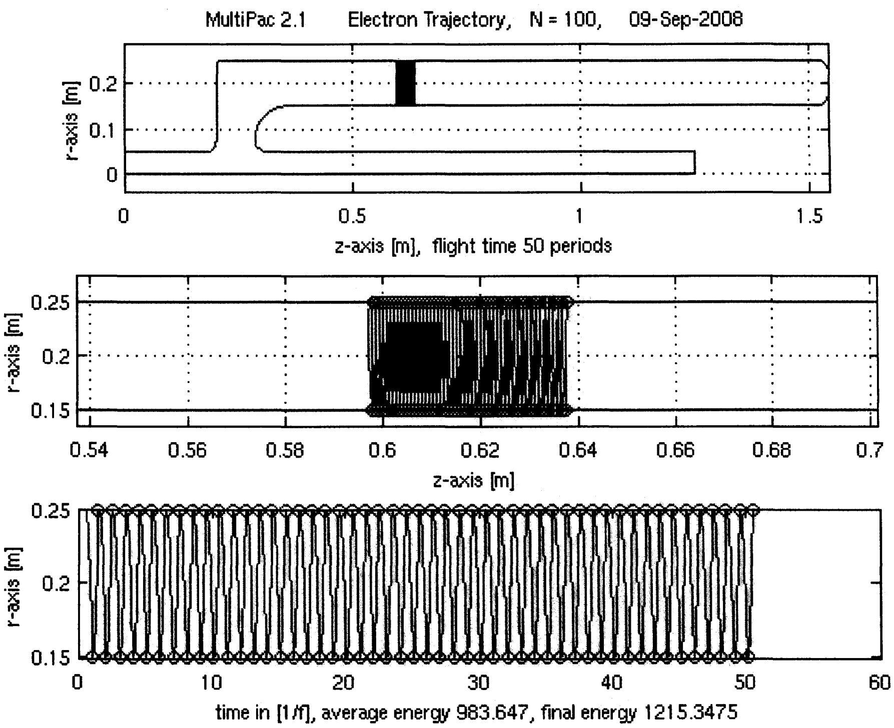
MultiPac 2.1 Electron Trajectory, N = 100, 09-Sep-2008
r-axis [m]
z-axis [m], flight time 50 periods
z-axis [m]
time in [1/f], average energy 983.647, final energy 1215.3475

(c)

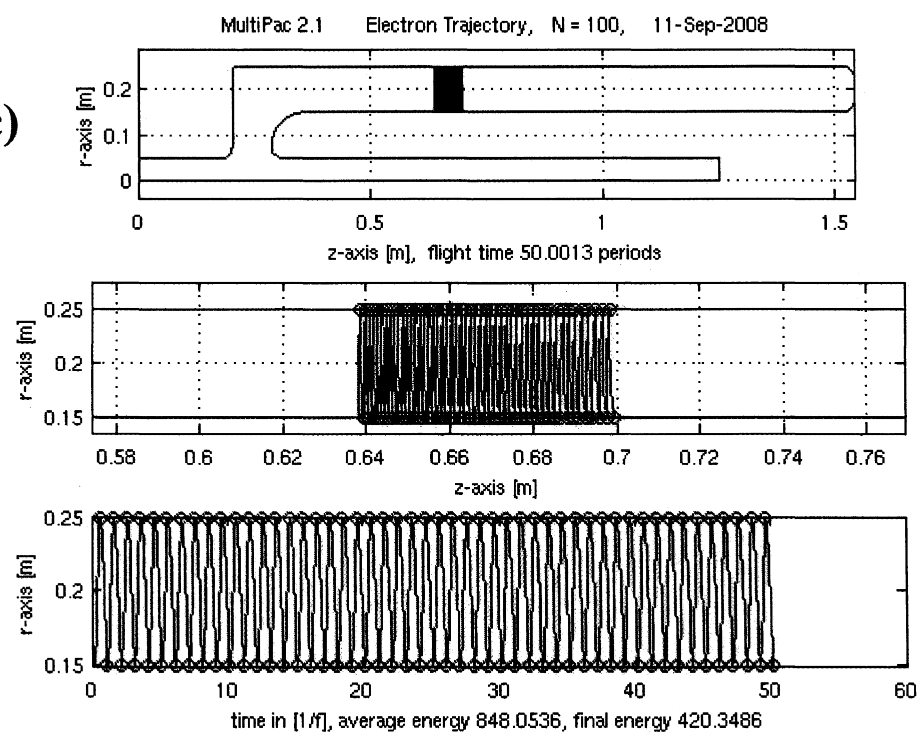
MultiPac 2.1 Electron Trajectory, N = 100, 11-Sep-2008
r-axis [m]
z-axis [m], flight time 50.0013 periods
z-axis [m]
time in [1/f], average energy 848.0536, final energy 420.3486

(d)

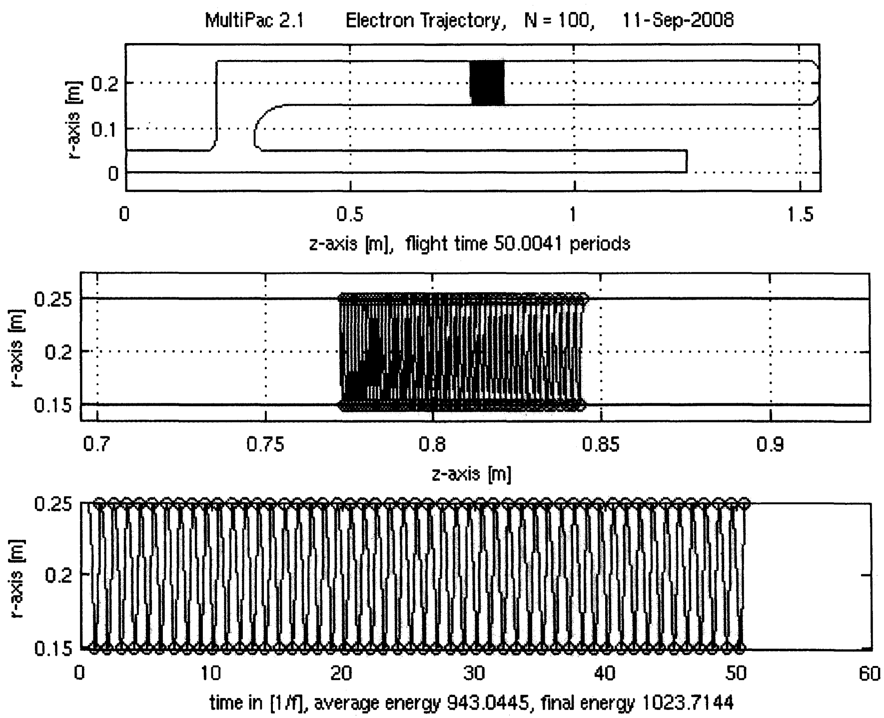
MultiPac 2.1 Electron Trajectory, N = 100, 11-Sep-2008
r-axis [m]
z-axis [m], flight time 50.0041 periods
z-axis [m]
time in [1/f], average energy 943.0445, final energy 1023.7144

(e)

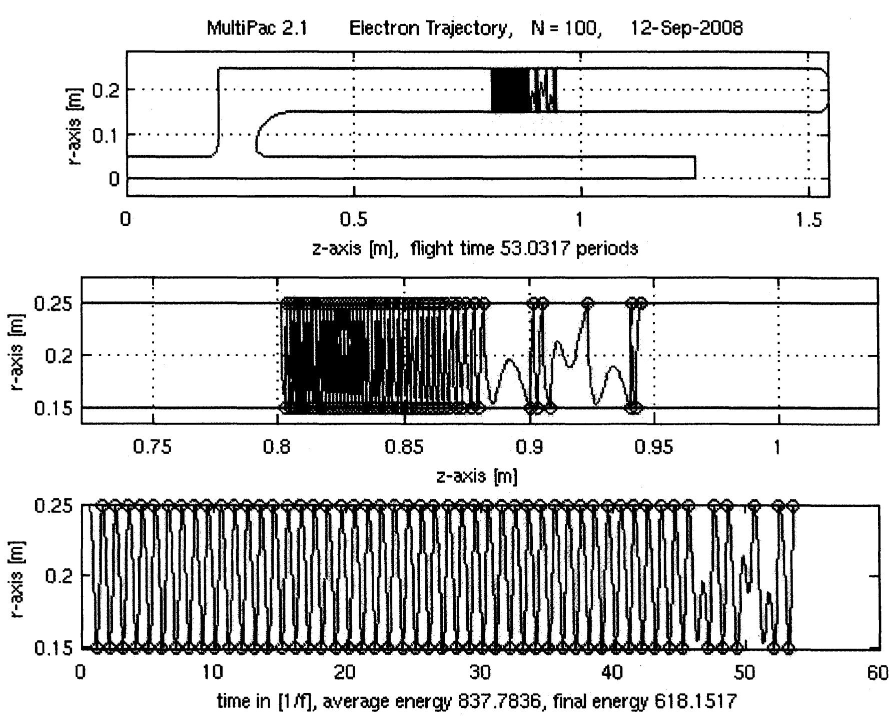
MultiPac 2.1 Electron Trajectory, N = 100, 12-Sep-2008
r-axis [m]
z-axis [m], flight time 53.0317 periods
z-axis [m]
time in [1/f], average energy 837.7836, final energy 618.1517

(f)

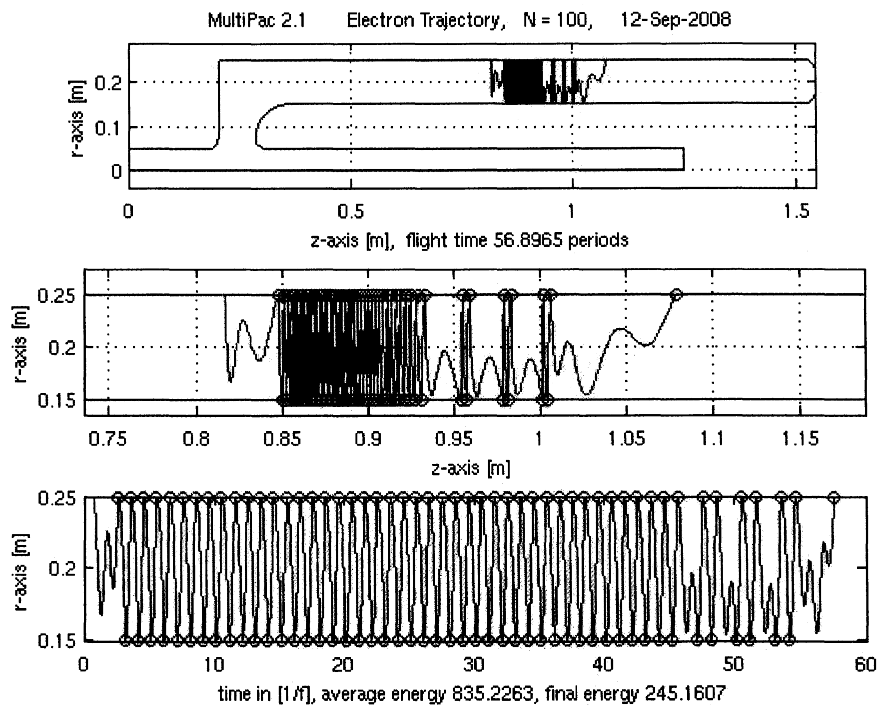

Fig.5. Electron trajectories for peak surface electric field (a) 36kV/m, (b, c) 40 kV/m, (d, e) 46kV/m and (f) 50kV/m.

3.1. Severity with electron impact more than 100: To assess the severity, the simulation was continued for more than 100 electron impacts and with some trajectories continuing for 500, 1000 or more times. Enhanced counter function also increases significantly indicating an intense electron cloud in the cavity (Fig. 6).

(a)

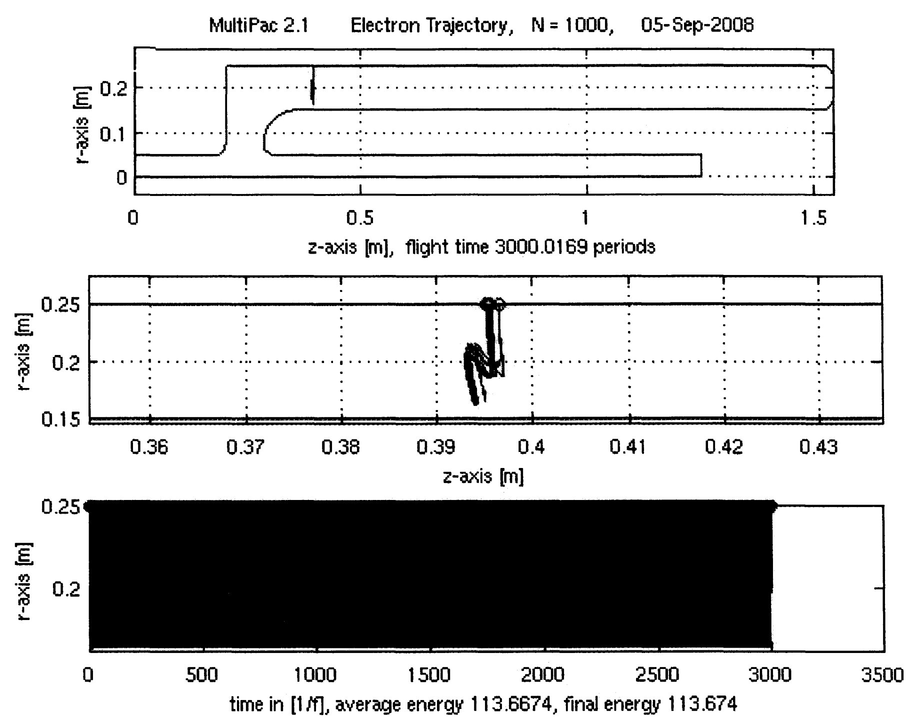

(b)

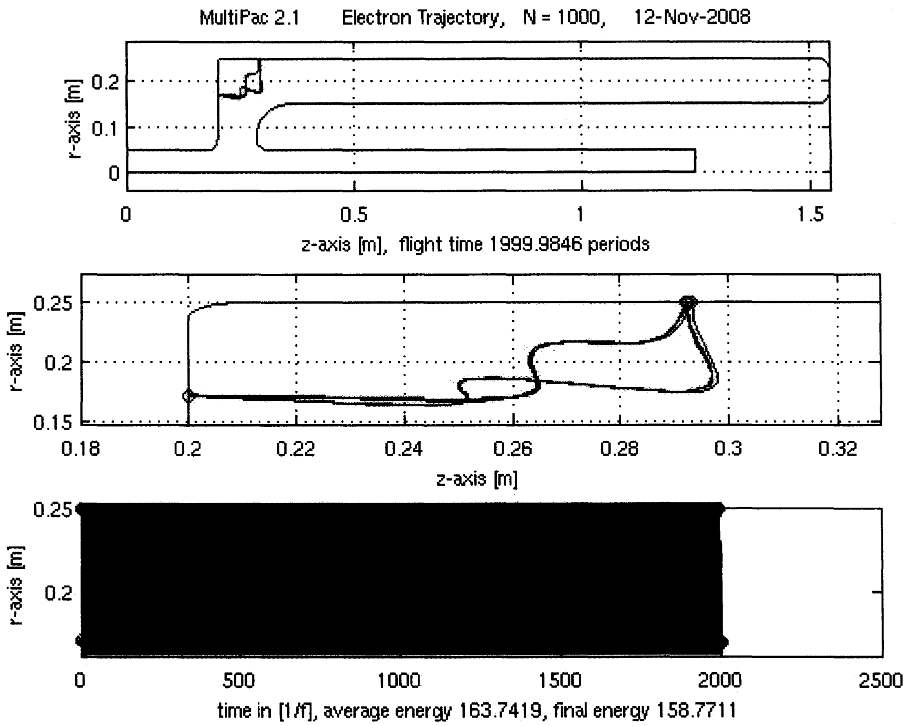

(c)

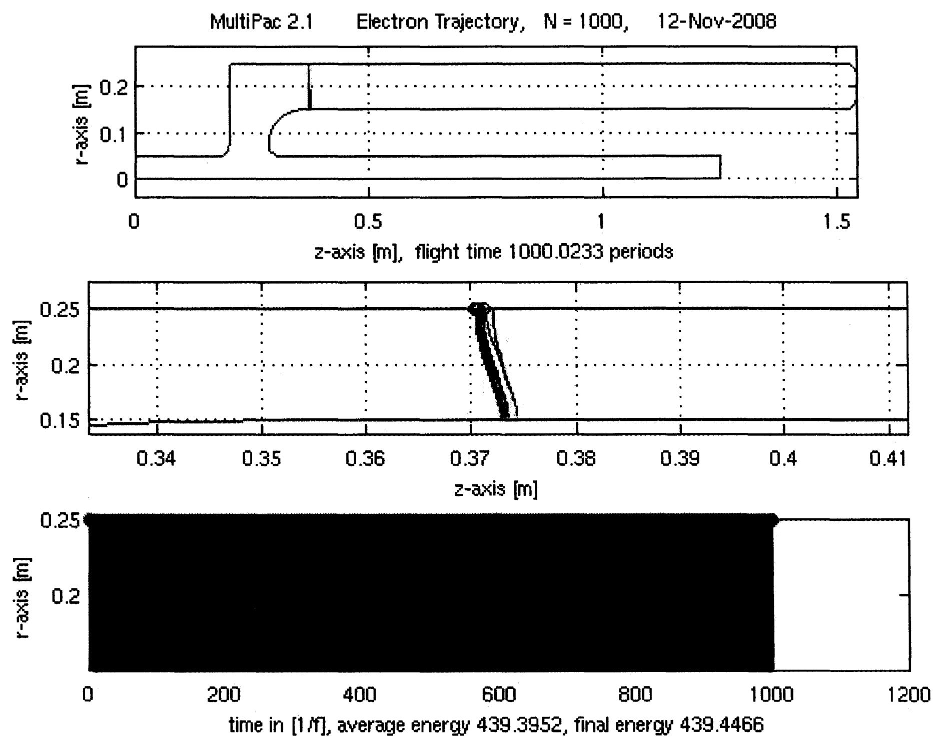

Fig.6. Some of the electron trajectories with 1000 impacts at peak surface electric field (a,c) 47 kV/m and (b) 31 kV/m.

4. Supression : The cavity cannot be operated safely in a storage ring when generating such a large number of electrons, so this phenomena must be suppressed. We reasoned that the most effective way to do so is by breaking the electron's stable resonant trajectory, thereby preventing its further multiplication irrespective of the cleanness of the niobium surface. While there are several approaches to control it from outside of the cavity (For example: by applying DC field) [2], due to complexity of the system and cryostat surrounding the cavity, they are not practical. As a useful alternative, structurally modifying the cavity was considered, and hence simulations were undertaken with various structures such as a bigger diameter of the outer conductor (Fig. 7), and also ripples pointing upward and downward direction in the outer conductor (Fig. 8).

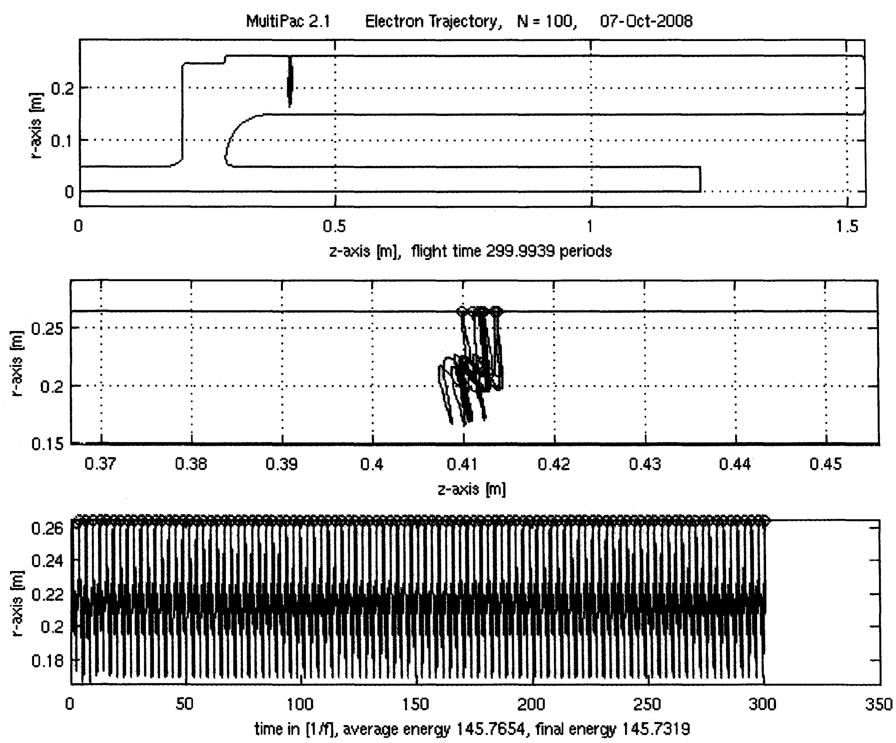

Fig. 7. Multipacting with bigger diameter (> 25cm) of outer conductor.

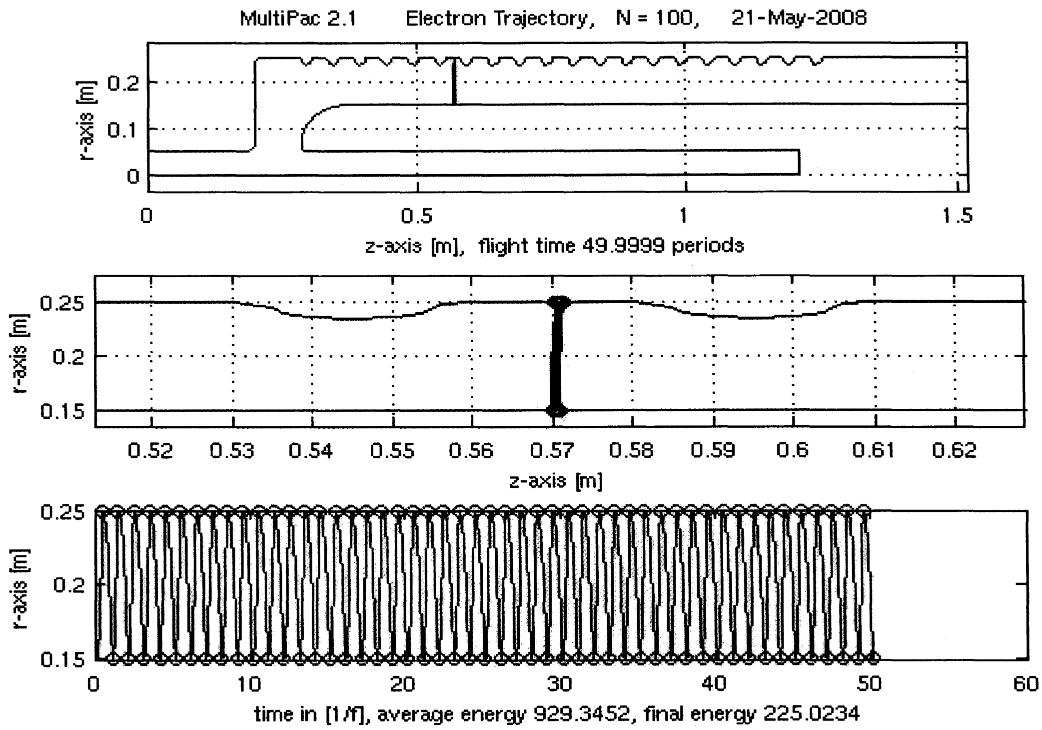

Fig. 8. Multipacting in the cavity when ripples point in the downward direction.

Among them the latter approach i.e incorporating ripples pointing in the upward direction seems to be the most promising (Fig. 9).

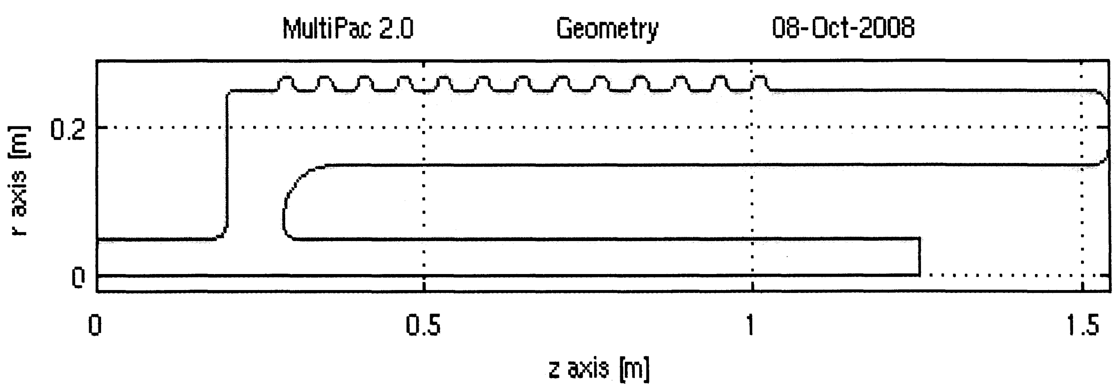

Fig. 9. Ripple pointing towards upward direction.

To reduce the manufacturing costs, the ripples are optimized to a customary depth, width, and ensure they are sufficiently separated. Also, they must leave sufficient space for coupler and dampers at the end of the cavity. Ripple depth up to 2 cm were considered for ripple width 1-3 cm, with the maximum possible separation between the ripple. The simulation revealed that for depth of 1 cm, the electron manages to have resonant trajectories in the ripple zone, moving further and further, and multiplying electrons. Constraints on the material's curvature also prohibit shallow ripples. However, ripples of 2 cm depths are found to be most valuable. The ripple's width also is critical. A 1 cm wide ripple is not satisfactory as electrons can emerge from it, whereas they undergo resonant oscillation inside a 3 cm ripple, and trapped there (Fig.10). Though the energy of the electrons are only few eV less ($\delta > 1$ at 55 eV) to have secondary electron yield greater than 1, a little impurity in Niobium, may lead to multipacting. Hence, 3 cm width should be avoided. However, 2 cm wide ripples are a good choice. Likewise it is essential

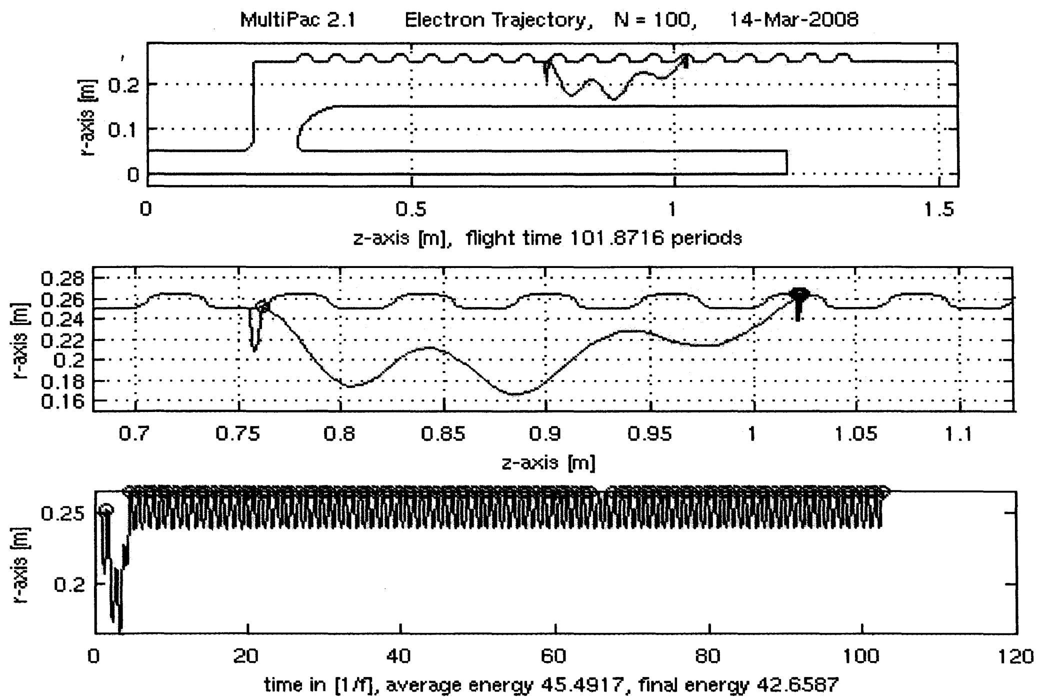

Fig. 10. Stable trajectrories of electrons inside a 3 cm wide ripple.

to determine the gap between the ripples. The stable trajectory of the electron is favored by having gaps bigger than 2 cm. Fig.11 depicts the stable electron trajectories for a gap of 4 cm between the ripples, whereas Fig.12 details the break in trajectory with 2 cm gap, even for 20 impacts.

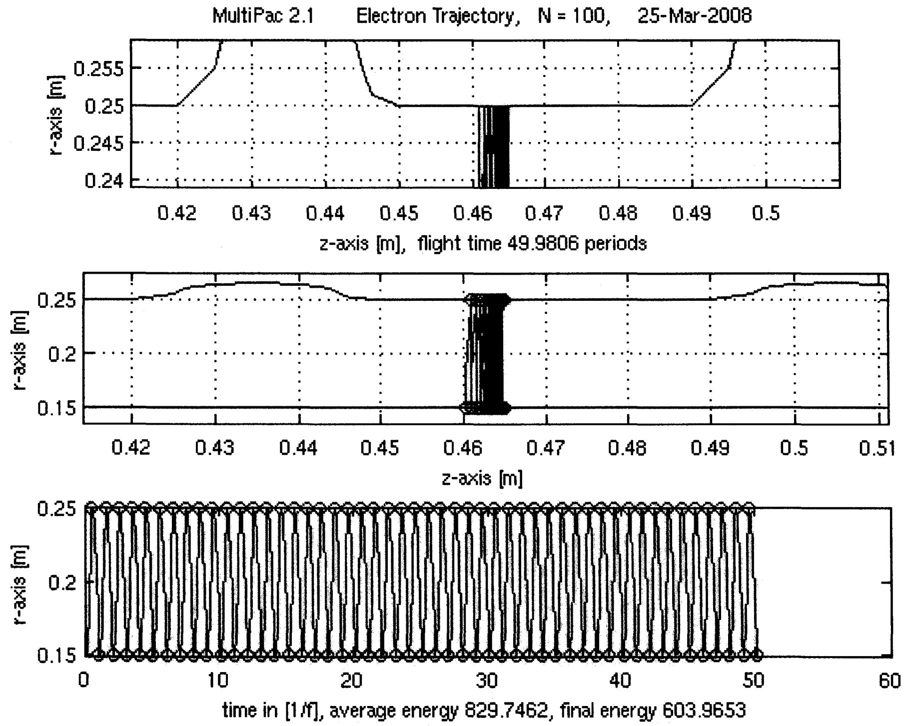

Fig. 11. Multipacting trajectory with 4 cm gap between the ripples.

Finally, it was demonstrated that ripples 2 cm deep, 2 cm wide with a 2 cm gap between them completely suppressed multipacting in the cavity; accordingly this approach was adopted for fabricating the cavity.

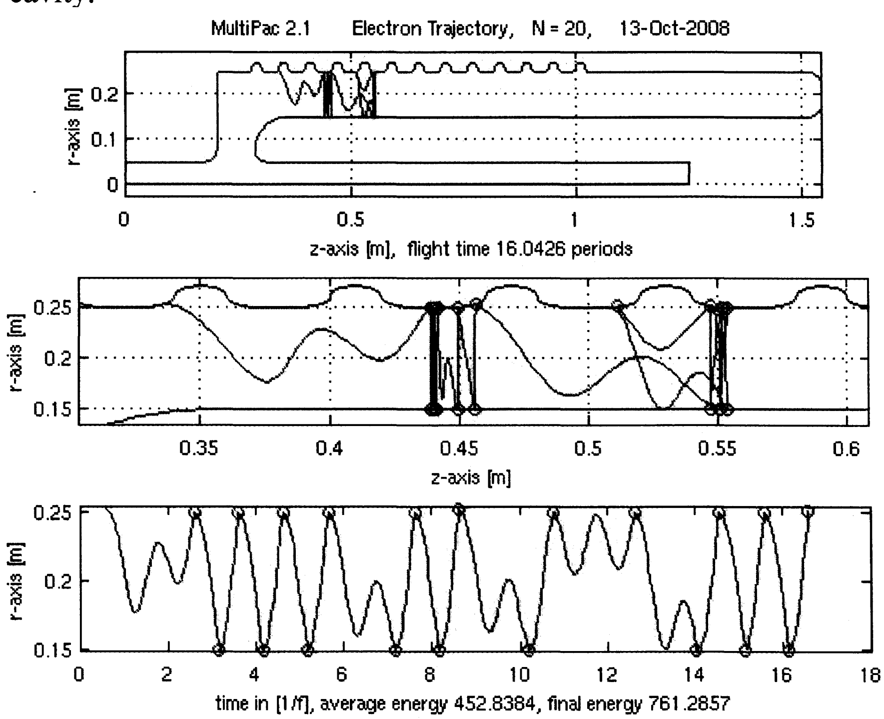

Fig. 12. Discontinuity of the resonance electron's trajectory with gap 2 cm between ripples, even for 20 impacts.

5. Conclusion: The 2D simulation revealed sever multipacting in 56 MHz QWR. We also show that multipacting can be eliminated in this cavity by structurally modifying its walls. Since the cavity is equipped with a coupler and dampers, which were omitted in the simulation, a further complete simulation is being carried out with a suitable 3D code to confirm the parameters for a multipacting free cavity revealed by this 2D code.

References:

[1] A.J. Hatch et. al, Phy. Rev. 112 (3) (1958) 681

[2] H. Padamsee, J. Knobloch, T. Hays. RF superconductivity for Accelerators.John Wiely and Sons Inc.

[3] http://www.bnl.gov/cad/ecooling/docs/PDF/56_MHz/Ben-Zvi.pdf

[4] http://conference.kek.jp/SRF2001/FA001.pdf